

### 3 Seepage

In this chapter the structure of soil particles within our two-phase continuum is considered to be *stationary* and effectively rigid, and we shall study the flow of water through it. This restriction means that we are investigating states of *steady flow* only, and we shall see in chapter 4 that *transient flow* implies change in effective stress which necessarily results in deformation of the soil matrix.

#### 3.1 Excess Pore-pressure

A simple apparatus for investigating the one-dimensional flow of water through a soil is the permeameter of Fig. 3.1. The apparatus consists of a perspex cylinder containing a soil specimen, in this case a saturated sand, supported by a gauze mesh with suitable size of aperture. De-aired water is supplied from a source at a constant head higher than the top of the permeameter, so that water is forced to flow upwards through the sand specimen.

Tappings at two neighbouring points, A and B, in the centre of the cylinder are connected with manometer tubes so that the pressures in the water can be recorded for both these points, with the level of the horizontal upper surface of the sand being used as datum.

Measuring  $z$  positively downwards, and  $h$  positively upwards from this datum, the *total* pressure in the pore-water  $u_w$  at A recorded by the manometer is simply  $u_w = \gamma_w(z + h)$ . Similarly, the *total* pressure at B is  $u_w + \delta u_w = \gamma_w(z + \delta z + h + \delta h)$ .

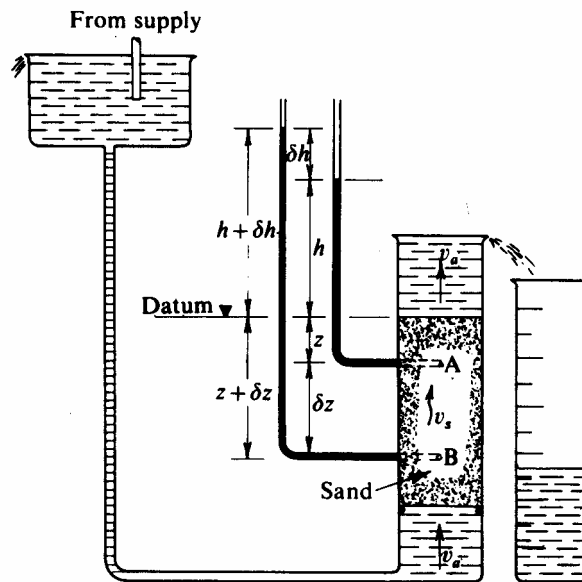


Fig. 3.1 Simple Permeameter

The difference between these two expressions

$$\delta u_w = \gamma_w(\delta z + \delta h) \quad (3.1)$$

is the difference in total pore-pressure between A and B and consists of two terms:

- a)  $\gamma_w \delta z$  which is the 'elevation' head, solely due to the difference in levels between A and B; it ensures that the total pressures are related to the same datum, and

- b)  $\gamma_w \delta h$  which will be denoted by  $\delta u$  and termed the *excess pore-pressure* between B and A; it is the sole cause of the (steady) flow of water upwards from B to A.

The quantity,  $\delta u$ , represents the energy loss per unit volume of water that flows from B to A; it is dissipated (a) in viscous drag as the water flows through the individual pores of the soil structure, and (b) in change of kinetic energy. In seepage problems in soil mechanics the latter term is negligible, and all the energy is effectively lost in drag, with corresponding reactions being generated in the soil structure, normally termed *seepage forces*.

### 3.2 Hydraulic Gradient

The points A and B have been chosen to be on the *same flowline* (i.e., water flows from one point on a flowline to the next) which happens to be vertical in this particular apparatus. Generally the flow will not be vertical, and Fig. 3.2 illustrates the case of seepage of groundwater where A and B are still neighbouring points on a flowline separated by a distance  $\delta s$  measured along the flowline but *against* the flow.

The *hydraulic gradient*  $i$  at the point A is a vector quantity defined to have magnitude

$$i = - \lim_{\delta s \rightarrow 0} \left( \frac{\delta h}{\delta s} \right) = - \frac{dh}{ds} = - \frac{1}{\gamma_w} \frac{du}{ds} \quad (3.2)$$

and to have direction of the flowline at A towards B. This choice of sign convention means that the hydraulic gradient is positive in the direction of the flow that it causes; and we need to note that it is a pseudo-dimensionless quantity, representing the space rate of energy loss per unit weight of water.

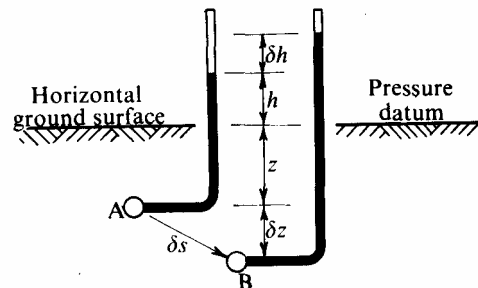


Fig. 3.2 Seepage of Groundwater

### 3.3 Darcy's Law

Darcy's law (1856) resulted from experiments to establish the relationship between hydraulic gradients and rates of flow of water. If  $Q$  is the volume of water flowing through the permeameter during time  $t$ , then the artificial (or approach and discharge) velocity  $v_a$  of the water is given by

$$v_a = \frac{Q}{A_t t}$$

where  $A_t$  is the *total* cross-sectional area of the interior of the perspex cylinder.

Darcy's law states that there is a linear relationship between hydraulic gradient and velocity for any given soil (representing a case of steady laminar flow at low Reynolds number)

$$v_a = ki = -k \frac{dh}{ds} \quad (3.3)$$

where the constant  $k$  is the coefficient of permeability (sometimes called the hydraulic conductivity) and has the dimensions of a velocity. Although the value of  $k$  is constant for a particular soil at a particular density it varies to a minor extent with viscosity and temperature of the water and to a major extent with pore size. For instance, for a coarse sand  $k$  may be as large as  $0.3 \text{ cm/s} = 3 \times 10^5 \text{ ft/yr}$ , and for clay particles of micron size  $k$  may be as small as  $3 \times 10^{-8} \text{ cm/s} = 3 \times 10^{-2} \text{ ft/yr}$ . This factor of  $10^7$  is of great significance in soil mechanics and is linked with a large difference between the mechanical behaviours of clay and sand soils.

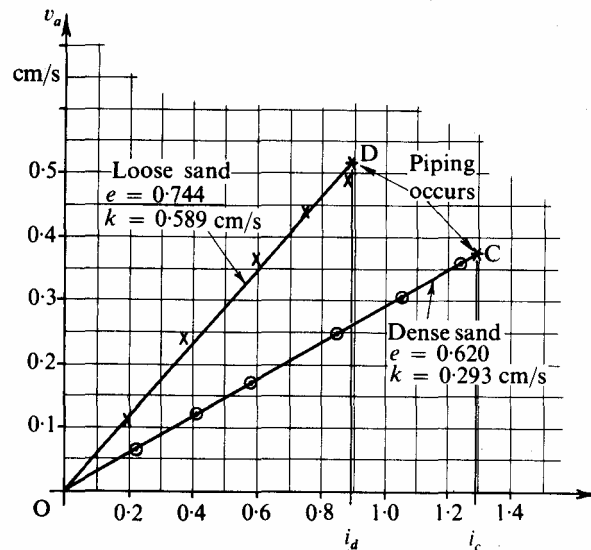


Fig. 3.3 Results of Permeability Test on Leighton Buzzard Sand

Typical results of permeability tests on a sample of Leighton Buzzard sand (between Nos. 14 and 25 B.S. Sieves) for a water temperature of  $20^\circ\text{C}$  are shown in Fig. 3.3. Initially the specimen was set up in a dense state achieved by tamping thin layers of the sand. The results give the lower straight line **OC**, which *terminates* at C. Under this hydraulic gradient  $i_c$  the upward drag on the particles imparted by the water is sufficient to lift their submerged weight, so that the particles float as a suspension and become a fluidized bed. This *quicksand* condition is also known as piping or *boiling*.

At this critical condition the total drag upwards on the sand between the levels of A and B will be  $A_t \delta u = A_t \gamma_w \delta h$  and this must exactly balance the submerged weight of this part of the sample, namely  $A_t \gamma' \delta s$ . Hence, the fluidizing hydraulic gradient should be given by

$$i_f = -\frac{dh}{ds} = +\frac{\gamma'}{\gamma_w} = \frac{G_s - 1}{1 + e}. \quad (3.4)$$

For the sand in question with  $e = 0.620$  (obtained by measuring the weight and overall volume of the sample) and  $G_s = 2.65$ , eq. (3.4), gives a critical hydraulic gradient of 1.02 which is an underestimate of the observed value of 1.29 (which included friction due to the lateral stresses induced in the sand sample in its preparation).

If during piping the supply of water is rapidly stopped the sand will settle into a very loose state of packing. The specific volume is correspondingly larger and the resulting permeability, given by line **OD**, has increased to  $k=0.589 \text{ cm/s}$  from the original value of  $0.293 \text{ cm/s}$  appropriate to the dense state. As is to be expected from eq. (3.4), the calculated value of the fluidizing hydraulic gradient has fallen to 0.945 because the sample

is looser; any increase in the value of  $e$  reduces the value of  $i_f$  given by eq. (3.4). We therefore expect  $i_c > i_d$ .

The variation of permeability for a given soil with its density of packing has been investigated by several workers and the work is well summarized by Taylor<sup>1</sup> and Harr<sup>2</sup>. Typical values for various soil types are given in Table 3.1.

<i>Soil type</i>	<i>Coefficient of permeability cm/sec</i>
Gravels	$k > 1$
Sands	$1 > k > 10^{-3}$
Silts	$10^{-3} > k > 10^{-6}$
Clays	$10^{-6} > k$

Table 3.1 Typical values of permeability

The actual velocity of water molecules along their narrow paths through the specimen (as opposed to the smooth flowlines assumed to pass through the entire space of the specimen) is called the seepage velocity,  $v_s$ . It can be measured by tracing the flow of dye injected into the water. Its average value depends on the unknown cross-sectional area of voids  $A_v$ , and equals  $Q/A_v t$ . But

$$v_s = \left( \frac{Q}{A_v t} \right) = \left( \frac{Q}{A_t t} \right) \left( \frac{A_t}{A_v} \right) = v_a \cdot \frac{V_t}{V_v} = \frac{v_a}{n} = v_a \left( \frac{1+e}{e} \right) \quad (3.5)$$

where  $V_t$  and  $V_v$  are the total volume of the sample and the volume of voids it contains, and  $n$  is the porosity. Hence, for the dense sand sample, we should expect the ratio of velocities to be

$$\frac{v_s}{v_a} = \frac{1+e}{e} = 2.62.$$

It is general practice in all seepage calculations to use the artificial velocity  $v_a$  and total areas so that consistency will be achieved.

### 3.4 Three-dimensional Seepage

In the last section dealing with Darcy's law, we studied the one-dimensional flow of water through a soil sample in the permeameter. We now extend these concepts to the general three-dimensional case, and consider the flow of pore-water through a small cubical element of a large mass of soil, as shown in Fig. 3.4. Let the excess pore-pressure at any point be given by the function  $u = f(x, y, z)$  which remains unchanged with time, and let the resolved components of the (artificial) flow velocity  $v_a$  through the element be  $(v_x, v_y, v_z)$ . Since the soil skeleton or matrix remains undeformed and the water is assumed to be incompressible, the bulk volume of the element remains constant with the inflow of water exactly matching the outflow. Remembering that we are using the artificial velocity and total areas then we have

$$v_x dy dz + v_y dz dx + v_z dx dy = \left( v_x + \frac{\partial v_x}{\partial x} dx \right) dy dz + \left( v_y + \frac{\partial v_y}{\partial y} dy \right) dz dx + \left( v_z + \frac{\partial v_z}{\partial z} dz \right) dx dy,$$

i.e.,

$$\frac{\partial v_x}{\partial x} + \frac{\partial v_y}{\partial y} + \frac{\partial v_z}{\partial z} = 0. \quad (3.6)$$

Darcy's law, so far established only for a flowline, is also applicable for resolved components of velocity and hydraulic gradient.

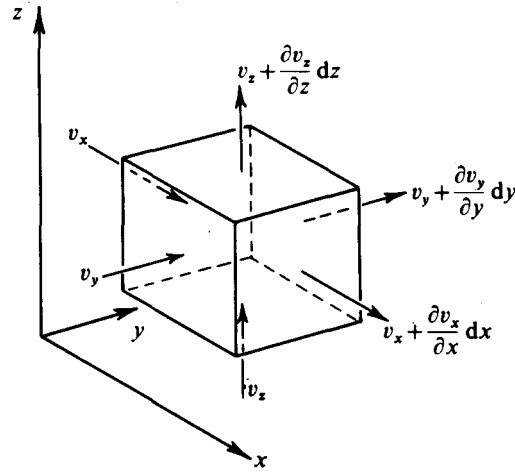


Fig. 3.4 Three-dimensional Seepage

In addition, it is possible for the permeability of the soil not to be isotropic, so that we have as the most general case

$$\left. \begin{aligned} v_x &= k_x i_x = -\frac{k_x}{\gamma_w} \frac{\partial u}{\partial x} \\ v_y &= k_y i_y = -\frac{k_y}{\gamma_w} \frac{\partial u}{\partial y} \\ v_z &= k_z i_z = -\frac{k_z}{\gamma_w} \frac{\partial u}{\partial z} \end{aligned} \right\} \quad (3.7)$$

and on substituting these equalities in eq. (3.6) we obtain

$$k_x \frac{\partial^2 u}{\partial x^2} + k_y \frac{\partial^2 u}{\partial y^2} + k_z \frac{\partial^2 u}{\partial z^2} = 0 \quad (3.8)$$

which is the general differential equation for the excess pore-pressure  $u(x, y, z)$  causing *steady* seepage in three dimensions.

Having derived this equation we have an exact analogy with the corresponding differential equations for the steady flow of electricity and heat through bodies, respectively

$$\begin{aligned} \frac{1}{R_x} \frac{\partial^2 V}{\partial x^2} + \frac{1}{R_y} \frac{\partial^2 V}{\partial y^2} + \frac{1}{R_z} \frac{\partial^2 V}{\partial z^2} &= 0 \\ C_x \frac{\partial^2 \Theta}{\partial x^2} + C_y \frac{\partial^2 \Theta}{\partial y^2} + C_z \frac{\partial^2 \Theta}{\partial z^2} &= 0 \end{aligned}$$

where  $V$  is the electric potential,  $R_x$ ,  $R_y$ , and  $R_z$  are electrical resistances,  $\Theta$  is the temperature, and  $C_x$ ,  $C_y$ , and  $C_z$  are thermal conductivities. Consequently, we can use these analogies for obtaining solutions to specific seepage problems.

### 3.5 Two-dimensional Seepage

In many real problems of soil mechanics the conditions are essentially two-dimensional, as in the case of seepage under a long sheet-pile wall or dam. We shall examine the former of these in the next section.

If we take the  $y$ -axis along the sheet-pile wall, there can be no flow or change in excess pore-pressure in the  $y$ -direction; hence  $\frac{\partial u}{\partial y} \equiv 0$ . We can further simplify the problem by taking  $k_x = k_z$ , because even if this is not the case, we can reduce the problem to its equivalent by distorting the scale in one direction.\* To do this we select a new transformed variable

$$x_t = \sqrt{\left(\frac{k_z}{k_x}\right)} x$$

so that the basic equation, (3.8), is reduced to

$$\frac{\partial^2 u}{\partial x_t^2} + \frac{\partial^2 u}{\partial z^2} = 0. \quad (3.9)$$

This equation (known as Laplace's equation) is satisfied by plane harmonic functions, which are represented graphically by two families of orthogonal curves; one family forms the equipotentials and the other the flowlines, as shown in Figs. 3.5 and 3.6.

However, there will not be many cases of particular boundary conditions for which eq. (3.9) will be exactly soluble in closed mathematical form, and we shall depend on the various approximate methods described in relation to the sheet pile example of the next section, 3.6.

### 3.6 Seepage Under a Long Sheet Pile Wall: an Extended Example

Figure 3.5 is a section of a sheet pile wall POP' forming one side of a long coffer dam built in a riverbed: the bed consists of a uniform layer of sand overlying a horizontal (impermeable) stratum. The analysis of the cofferdam for any given depth of driving could pose the problems of the quantity of seepage that can be expected to enter the working area from under the wall, or the stability against piping which will be most critical immediately behind the wall. Approximate answers could be obtained from the following alternative methods:

(a) *Model experiment in the laboratory.* A model of the riverbed is constructed in a narrow tank with glass or perspex sides which are perpendicular to the sheet pile. The different water levels on each side are kept constant, with the downstream level being just above the sandbed to ensure saturation. Probes are placed through these transparent sides at convenient positions, as for the permeameter, to record the excess pore-pressures and thereby indicate the equipotentials. The flowlines can readily be obtained by inserting small quantities of dye at points on the upstream surface of the sand (against one of the transparent faces of the tank) and tracing their subsequent paths. We can also measure the quantity of seepage that occurs in a given time.

There will be symmetry about the centre line P'OP and the imposed boundary conditions are that (i) the upper surface of the sand on the upstream side, AO, is an equipotential  $\phi = h$ , (ii) the upper surface of the sand on the downstream side, OB, is also an equipotential  $\phi = 0$ , (iii) the lower surface of the sand is a flowline, and (iv) the buried surface of the sheet pile itself is a flowline. Readings obtained from such a laboratory model have been used to give Fig. 3.5.

\* For full treatment of this topic, reference should be made to Taylor<sup>1</sup> or Harr<sup>2</sup> however, it should be noted that these authors differ in their presentation. Taylor's flownets consist of conjugate functions formed by equipotentials of *head* and of *flux*, whereas Harr's approach has conjugate functions of equal values of *velocity potential* and of *velocity*. There is, in effect, a difference of a factor of permeability between these two approaches which only becomes important for a soil with anisotropic permeability. Here we have an isotropic soil and this distinction need not concern us.

(b) *Electrical analogue.* A direct analogue of the model can be constructed by cutting out a thin sheet of some suitable conducting material to a profile identical to the section of the sand including a slit, OP, to represent the sheet pile. A potential is applied between the edges AO and OB; and equipotentials can be traced by touching the conducting sheet with an electrical probe connected to a Wheatstone bridge.

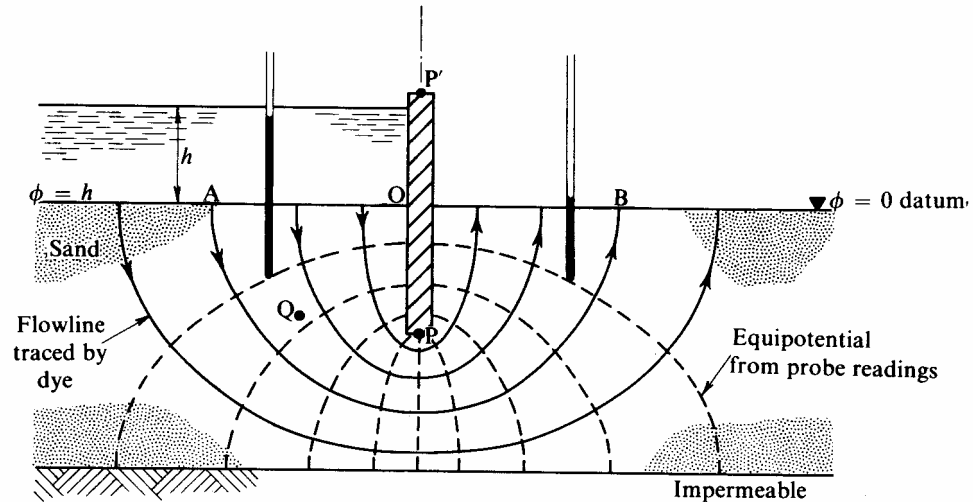


Fig. 3.5 Seepage under Model of Long Sheet Pile Wall

Unlike method (a) above, we cannot trace separately the flow-lines of current. This method can be extended to the much more complicated case of three-dimensional seepage by using an electrolyte as the conducting material.

(c) *Graphical flownet.* It is possible to obtain a surprisingly accurate two-dimensional flownet (corresponding to that of Fig. 3.5) by a graphical method of trial and error. Certain guiding principles are necessary such as the requirement that the formation of the flownet is only proper when it is composed of 'curvilinear squares': these will not be dealt with here, but are well set out in Taylor's book.<sup>1</sup>

(d) *Relaxation methods.* These are essentially the same as the graphical approach of (c) to the problem, except that the construction of the correct flownet is semi-computational.

### 3.7 Approximate Mathematical Solution for the Sheet Pile Wall

The boundary conditions of the problem of §3.6 are such that with one relatively unimportant modification an exact mathematical solution can be obtained. This modification is that the sandbed should be not only of infinite extent laterally but also in depth as shown in Fig. 3.6. In this diagram we are taking  $OB_1B_2$  as the x-axis and  $OPC_1C_2$  as the z-axis, and adopting for convenience a unit head difference of water between the outside and inside of the cofferdam; we are taking as our pressure datum the mean of these two, so that the upstream horizontal equipotential  $\phi = +\frac{1}{2}$ , and the downstream one is  $\phi = -\frac{1}{2}$ . The buried depth of sheet pile is taken as  $d$ .

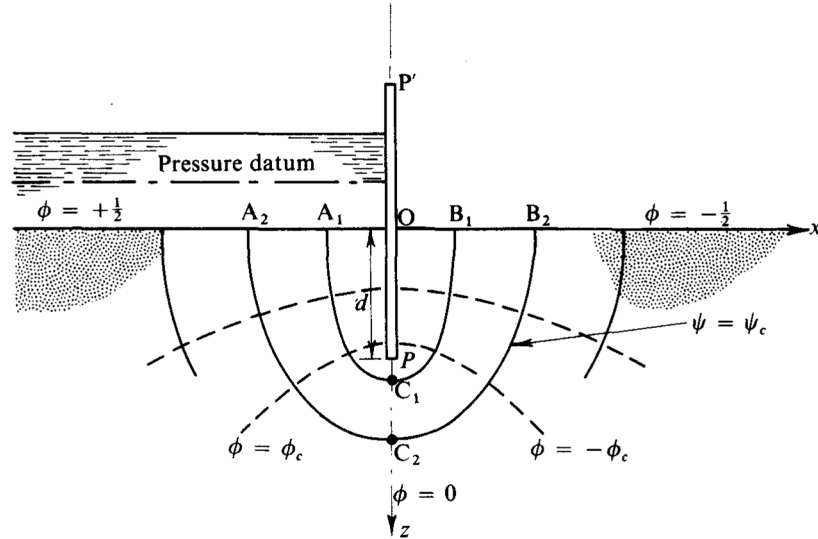


Fig. 3.6 Mathematical Representation of Flownet

We need to find conjugate functions  $\phi(x, z)$  and  $\psi(x, z)$  of the general form  $(\phi + i\psi) = f(z + ix)$  that satisfy the boundary conditions of our particular problem; the Laplace differential equation, (3.9), will automatically be satisfied by such conjugate functions. (Differentiating we have

$$\frac{\partial \phi}{\partial z} + i \frac{\partial \psi}{\partial z} = f' \quad \text{and} \quad \frac{\partial \phi}{\partial x} + i \frac{\partial \psi}{\partial x} = if'$$

so that

$$\frac{\partial \phi}{\partial z} = + \frac{\partial \psi}{\partial x} \quad \text{and} \quad - \frac{\partial \psi}{\partial z} = \frac{\partial \phi}{\partial x}$$

Differentiating again

$$\frac{\partial^2 \phi}{\partial z^2} + i \frac{\partial^2 \psi}{\partial z^2} = f'' = - \left( \frac{\partial^2 \phi}{\partial x^2} + i \frac{\partial^2 \psi}{\partial x^2} \right)$$

from which we have

$$\frac{\partial^2 \phi}{\partial x^2} + \frac{\partial^2 \phi}{\partial z^2} = 0 = - \left( \frac{\partial^2 \psi}{\partial x^2} + \frac{\partial^2 \psi}{\partial z^2} \right)$$

i.e., Laplace's equation is satisfied.)

Consider the relationship

$$\pi(\phi + i\psi) = \cos^{-1} \frac{(z + ix)}{d} \quad (3.10)$$

i.e.,

$$\frac{z + ix}{d} = \cos \pi(\phi + i\psi) = \cos \pi\phi \cosh \pi\psi - i \sin \pi\phi \sinh \pi\psi.$$

Equating real and imaginary parts

$$\left. \begin{aligned} x &= -d \sin \pi\phi \sinh \pi\psi \\ z &= d \cos \pi\phi \cosh \pi\psi. \end{aligned} \right\} \quad (3.11)$$

Eliminating  $\phi$  we obtain

$$\frac{x^2}{d^2 \sinh^2 \pi\psi} + \frac{z^2}{d^2 \cosh^2 \pi\psi} = 1 \quad (3.12)$$



which defines a family of confocal ellipses, each one being determined by a fixed value of  $\psi = \psi_c$  and describing a streamline. The joint foci are given by the ends of the limiting ‘ellipse’  $\psi = 0$  which from eq. (3.11) are  $x = 0, z = \pm d$ .

Similarly, eliminating  $\psi$  we obtain

$$\frac{z^2}{d^2 \cos^2 \pi\phi} + \frac{x^2}{d^2 \sin^2 \pi\phi} = 1 \quad (3.13)$$

which defines a family of confocal hyperbolae, each one being determined by a fixed value of  $\phi = \phi_c$  and describing an equipotential. The limiting ‘hyperbola’ corresponding to  $\phi = 0$  leads to the same foci as for the ellipses.

We have yet to establish that the boundary conditions are exactly satisfied, which will now be done.

For  $x = 0$  eq. (3.11) demands that either

$$\psi = 0$$

leading to,  $z = d \cos \pi\phi$ , i.e., P’OP; or

$$\phi = 0$$

leading to  $z = d \cosh \pi\psi$ , i.e., **PZ** (or positive z-axis below P).

(The possibility of  $\phi = 1$  gives the negative z-axis above P’.)

For  $z = 0$  eq. (3.11) demands that either

$$\phi = \frac{1}{2}$$

leading to  $x = -d \sinh \pi\psi$ ; or

$$\phi = -\frac{1}{2}$$

leading to  $x = d \sinh \pi\psi$ .

If we arbitrarily restrict  $\psi$  to being positive then

$$\phi = \frac{1}{2}, \psi \geq 0 \quad \text{gives the negative } x\text{-axis } OA_1A_2$$

$$\phi = -\frac{1}{2}, \psi \geq 0 \quad \text{gives the positive } x\text{-axis } OB_1B_2.$$

We have therefore established a complete solution, and in effect if we plot the result in the  $(\phi, \psi)$  plane in Fig. 3.7 we see that we have re-mapped the infinite half plane of the sand into the infinitely long thin rectangle. This process is known as a conformal transformation, and has transformed the flownet into a simple rectilinear grid. In particular it can be seen that the half ellipse *with slit*  $POA_1A_2C_2B_2B_1OP$  has been distorted into the rectangle  $PO_1A'_2B'_2O_2P$  and the process can be visualized in Fig. 3.7 as a simultaneous rotation in opposite directions of the top corners of the slit about the bottom, P.

At any general point **Q** of the sandbed the hydraulic gradient is given by  $-\left(\frac{d\phi}{ds}\right)$  which in *magnitude* (but not necessarily sign) equals

$$|\text{grad } \phi| = \sqrt{\left\{\left(\frac{\partial \phi}{\partial x}\right)^2 + \left(\frac{\partial \phi}{\partial z}\right)^2\right\}}$$

where  $s$  is measured ‘up’ a streamline. Appropriate differentiation and manipulation of eqs. (3.11) leads to the expression

$$|i| = \frac{1}{\pi d \sqrt{\sinh^2 \pi\psi + \sin^2 \pi\phi}} = \frac{1}{\pi \left\{ (d^2 + x^2 - z^2)^2 + 4x^2 z^2 \right\}^{\frac{1}{4}}}. \quad (3.14)$$

Hence we can calculate the hydraulic gradient and resulting flow velocity at any point in the sandbed, and compare the predictions with experimental values obtained from the model.

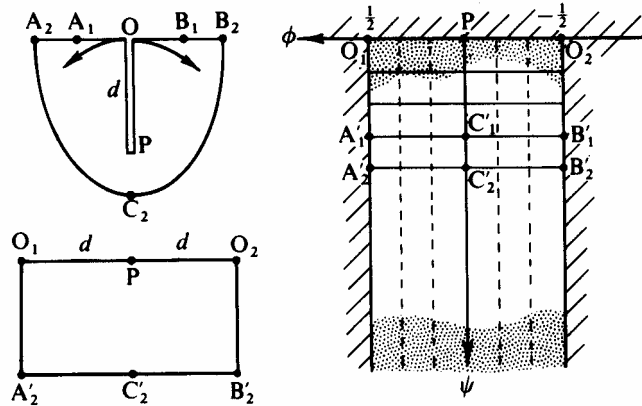


Fig. 3.7 Transformed Flownet

Typical experimental readings obtained from the laboratory model are:

Depth of sheet pile in sand = 6.67 in.; depth of sand bed 12 in.; breadth of model  $b = 6.55$  in.; upstream head of water  $h = 3.85$  in.; average voids ratio of sand  $e = 0.623$  for which the specific gravity  $G_s = 2.65$  and the permeability  $k = 0.165$  in./s; rate of seepage  $Q = 1.75$  in.<sup>3</sup>/s; and time for dye to travel from  $x = -5$ ,  $z = 7$  to  $x = -3.7$ ,  $z = 8$  was 30 s.

(a) *Comparison of seepage velocity.* The coordinates of Q, the mean point of the measured dye path, are  $x = -4.35$ ,  $z = 7.5$  and substituting in eq. (3.14) we get for *unit head*  $|i_q| = \frac{1}{\pi} \times 8.1$ . Hence predicted *seepage velocity* at Q will be

$$\begin{aligned} v_s &= \frac{v}{n} = \frac{v(1+e)}{e} = k|i_q|h \frac{(1+e)}{e} \\ &= \frac{0.165 \times 3.85 \times 1.623}{\pi \times 8.1 \times 0.623} = 0.065 \text{ in./s.} \end{aligned}$$

This compares with a measured value of

$$\frac{\sqrt{(1^2 + 1.3^2)}}{30} = 0.0547 \text{ in./s.}$$

and is an overestimate by 18 per cent.

(b) *Total seepage.* The mathematical solution gives an infinite value of seepage since the sand bed has had to be assumed to be of infinite depth. But as a reasonable basis of comparison we can compute the seepage passing under the sheet pile,  $z = d$ , down to a depth  $z = 1.8d$  which corresponds with the bottom of the sand in the model. This is equivalent to taking the boundary of the sand as a half ellipse such as  $A_2C_2B_2$  where  $OC_2 = 1.8d$ .

$$Q = \int_d^{1.8d} v_a b dz = kbh \int_d^{1.8d} \frac{i}{h} dz.$$

But on the line  $x = 0$ , the streamlines are all in the positive  $x$ -direction and  $i/h = +\partial\phi/\partial s = -\partial\phi/\partial x$  since  $\delta s = -\delta x$ , and the properties of the conjugate functions are such that  $\partial\phi/\partial x = -\partial\psi/\partial z$ .

Hence,

$$Q = kbh \int_d^{1.8d} \frac{\partial\psi}{\partial z} dz = kbh[\psi]_{z=d}^{z=1.8d} = \frac{kbh}{\pi} \left[ \cosh^{-1}\left(\frac{z}{d}\right) \right]_d^{1.8d}$$

$$= \frac{0.165 \times 6.55 \times 3.85 \times 1.195}{\pi} = 1.59 \text{ in.}^3 / \text{s}.$$

This compares with a measured value of 1.75 in.<sup>3</sup>/s and is as expected an underestimate, by an order of 9 per cent.

The effect of cutting off the bottom of the infinite sand bed below a depth  $z = 1.8d$  in the model, is to crowd the flowlines closer to the sheet-pile wall; consequently, we expect in the model a higher measured seepage velocity and a higher total seepage. The comparatively close agreement between the model experiment and the mathematical predictions is because the modification to the boundary conditions has little effect on the flownet where it is near to the sheet pile wall and where all the major effects occur.

A further important prediction concerns the stability against piping. The predicted hydraulic gradient at the surface of the sand immediately behind the sheet-pile wall ( $\psi = 0, \phi = -\frac{1}{2}$ ) is  $h/\pi d$ . Hence the predicted factor of safety against piping under this difference of head is

$$\frac{\gamma'}{i\gamma_w} = \frac{(G_s - 1)}{\left(\frac{h}{\pi d}\right)(1 + e)} = \frac{1.65 \times \pi \times 6.67}{3.85 \times 1.623} = 5.5.$$

### 3.8 Control of Seepage

In the previous sections we have explained the use of a conceptual model for seepage: the word 'model' in our usage has much the same sense as the word 'law' that was used a couple of hundred years ago by experimental workers such as Darcy. We only needed half a chapter to outline the simple concepts and formulate the general equations, and in the rest of the chapter we have gone far enough with the solution of a two-dimensional problem to establish the status of the seepage problem in continuum mechanics. Rather than going on to explain further techniques of solution, which are discussed by Harr<sup>2</sup>, we will turn to discuss the simplifications that occur when a designer controls the boundaries of a problem.

Serious consequences may attend a failure to impound water, and civil engineers design major works against such danger. There is a possibility that substantial flow of seepage will move soil solids and form a pipe or channel through the ground, and there is also danger that substantial pore-pressures will occur in ground and reduce stability even when the seepage flow rate is negligibly small. The first risk is reduced if a *graded filter* drain is formed in the ground, in which seepage water flows under negligible hydraulic gradient. The materials of such filters are sands and gravels, chosen to be stable against solution, and made to resist movement of small particles by choosing a succession of gradings which will not permit small particles from any section of the filter to pass through the voids of the succeeding section.

These *drains* have a most important role in relieving pore-pressure and, for example, reducing uplift below a dam: wells serve the same function when used to lower

groundwater levels and prevent artesian pressure of water in an underlying sand layer bursting the floor of an excavation in an overlying clay layer. The technical possibilities could be to insert a porous tipped pipe and cause local spherical flow, or to insert a porous-walled pipe and cause local radial flow, or to place or insert a porous-faced layer and cause local parallel flow. These three possibilities correspond to more simple solutions than the two-dimensional problem discussed above:

(a) The Laplace equation for spherical flow is

$$\frac{1}{r^2} \frac{\partial}{\partial r} \left( r^2 \frac{\partial h}{\partial r} \right) = 0$$

which can be integrated to give

$$(h_1 - h_2) \propto \left( \frac{1}{r_2} - \frac{1}{r_1} \right);$$

and (b) the Laplace equation for radial flow is

$$\frac{1}{r} \frac{\partial}{\partial r} \left( r \frac{\partial h}{\partial r} \right) = 0$$

which can be integrated to give

$$(h_1 - h_2) \propto \ln \left( \frac{r_1}{r_2} \right)$$

and (c) the Laplace equation for parallel flow is

$$\frac{\partial^2 h}{\partial r^2} = 0$$

which can be integrated to give

$$(h_1 - h_2) \propto (r_1 - r_2);$$

where  $(h_1 - h_2)$  is the loss of head between coordinates  $r_1$  and  $r_2$ .

A contrasting technical possibility is to make a layer of ground relatively impermeable. Two or three lines of holes can be drilled and grout can be injected into the ground; a trench can be cut and filled with clay slurry or remoulded 'puddled' clay; or a blanket of rather impermeable silty or clayey soil can be rolled down. Seepage through these *cut-off* layers is calculated as a parallel flow problem.

In 'seepage space' a cut-off is immensely large and a drain is extremely small. The designer can vary the spatial distribution of permeability and adjust the geometry of seepage by introducing cut-offs and drains until the mathematical problem is reduced to simple calculations. Applied mathematics can play a useful role, but engineers often carry solutions to slide-rule accuracy only and then concentrate their attention on (a) the actual observation of pore-pressures and (b) the actual materials, their permeabilities, and their susceptibility to change with time.

### References to Chapter 3

- <sup>1</sup> Taylor, D. W. *Fundamentals of Soil Mechanics*, Wiley, 1948.
- <sup>2</sup> Harr, M. E. *Groundwater and Seepage*, McGraw-Hill, 1962.